Theory of dressed-state lasers. II. Phase diffusion and squeezing

Jakub Zakrzewski
Institute of Physics, Jagiellonian University, Reymonta 4, 30-059 Kraków, Poland

Maciej Lewenstein
Institute for Theoretical Physics, Polish Academy of Sciences, 02-668 Warsaw, Poland

Thomas W. Mossberg
Department of Physics, University of Oregon, Eugene, Oregon 97403
(Received 26 December 1990)

We present a detailed theory of the quantum-statistical properties of dressed-state lasers, i.e., lasers that operate due to the gain on an inverted transition between dressed states of a coupled atom-field system. With the help of quantum Langevin equations, we calculate squeezing spectra of such lasers. One-photon dressed-state lasers exhibit large squeezing due to antiresonant transitions between dressed states that lead to Bloch-Siegert-type shift effects. Two-photon dressed-state lasers may also generate squeezed light.

PACS number(s): 42.50.Hz, 42.55.−f, 42.50.Kb

I. INTRODUCTION

This paper is the second in a series of works on the theory of dressed-state lasers. Dressed-state lasers [1] operate as a result of gain on inverted transitions between dressed states of a coupled atom-field system. Such physical situations arise when an ensemble of two-level atoms is driven by a strong nearly resonant laser field. The atoms are dressed by the laser field, and they may exhibit gain at frequencies corresponding to one-, two-, or multiphoton transitions between the dressed states. When a sufficiently large number of atoms are placed in a cavity that is tuned to a transition exhibiting gain, lasing may occur. In fact, one-photon dressed-state lasing has recently been observed [2].

In the preceding paper, effective Hamiltonians were derived and utilized to provide a detailed semiclassical description of dressed-state lasers [3]. In the effective Hamiltonian describing one-photon dressed-state lasing, we included terms corresponding to Bloch-Siegert-type [4] shifts of the dressed-state energies. These frequency corrections, while negligible compared to optical frequencies, are important in comparison to the effective Rabi frequency Ω', which measures the frequency difference between the dressed-state sublevels. We have shown that driven two-level atoms provide a promising gain medium for observation of the two-photon lasing in the optical regime. We have discussed carefully the competition between the resonant two-photon process and off-resonant one-photon lasing, showing how robust the first of these processes is. This paper is devoted to a study of the quantum-statistical properties of dressed-state lasers.

The problem of quantum fluctuations of laser radiation has been the subject of numerous studies since the 1960s [5]. In the recent years, this problem has been most frequently investigated with the help of the quasiprobability method [6]. Quantum fluctuations of lasers are described within this framework with help of Fokker-Planck-type equations [7] for quasiprobability functions. In the original approaches, Glauber's P representation was used [8]. Recently, however, other approaches, based on the Q function, Wigner function, and the positive or complex P representation, have been developed [9].

In the standard one-photon laser, quantum effects, such as photon antibunching [9], have been shown to be rather small. To a very good approximation, the photon statistics of a one-photon laser are Poissonian and correspond to those of a coherent state [6]. Two-photon lasers, on the other hand, are known to exhibit quantum squeezing effects [10,11], provided they are coherently pumped [12]. Squeezing is often described in terms of a squeezing spectrum $S(\omega)$ [13]. Negative values of $S(\omega)$ indicate intrinsic quantum effects. Modern techniques of evaluating $S(\omega)$ are also based on the quasiprobability approach, and typically they employ positive P, complex P, or standard P representations [14].

One should stress that in the stationary state incoherently driven optical systems, such as the single-mode laser, typically have some kind of a phase invariance. Thus fluctuations inevitably lead to phase diffusion [5], which in the long-time limit smears out any squeezing effects and leads to a uniformly positive squeezing spectrum $S(\omega)$. In fact, the squeezing spectrum becomes proportional to the power spectrum of the laser. One might think that the squeezing spectrum concept does not apply particularly well to such systems. This is not the case, however, since there are several methods of avoiding the coherence destroying effect of phase diffusion.

Typically, phase diffusion in lasers occurs on a very-long-time scale well separated from all the other time scales of the system. One can thus measure transient squeezing spectra [15] by limiting observation times to intervals much shorter than the inverse of the phase

diffusion constant.

We shall calculate below the squeezing spectra for dressed-state lasers, using quantum Langevin equations [16]. In Sec. II we present a brief description of our method, applied to the two-photon laser. Quantum Langevin equations in the dressed-state basis are derived there. We linearize these equations around stationary semiclassical solutions, describing dressed-state lasing. The discussion of phase diffusion and its influence on the squeezing spectrum is included in Secs. III and IV, respectively. Section V contains a discussion of our results for both one- and two-photon dressed-state lasers. The most fascinating result is that the one-photon dressed-state laser may exhibit large squeezing entirely as a result of antiresonant transitions between dressed states that lead to Bloch-Siegert shifts of the dressed-state energies. The two-photon dressed-state laser also exhibits considerable squeezing effects. Technical details of our calculations are presented in Appendixes A and B. This paper is followed by a third one [17], in which we discuss depletion effects of the pump (dressing) laser beam.

II. QUANTUM LANGEVIN EQUATIONS FOR DRESSED-STATE LASERS

In this section we shall begin our discussion of the quantum-statistical properties of dressed-state lasers. We use a method that is based on the quantum Langevin equations, but is slightly different from methods previously discussed in the literature [5,16]. We give details of the method as applied to the case of the two-photon laser only, since the expressions we derive can be easily transformed to describe the one-photon laser.

As a preface, we briefly recall the terminology of Ref. [1]. Two-level atoms of transition frequency ω_a are driven by a monochromatic pump field of frequency ω_L. The atoms are within a cavity having an isolated resonance at the frequency ω_c with a half width at half maximum of Γ. We let $\Delta_1=\omega_a-\omega_L$ and $\Delta_2=\omega_c-\omega_L$. The pump field has a resonant Rabi frequency of Ω and a generalized Rabi frequency of $\Omega'=(\Omega^2+\Delta_1^2)^{1/2}$. We also define the angle α by the relations $\Omega=\Omega'\sin 2\alpha$ and $\Delta_1=\Omega'\cos 2\alpha$.

In the quantum Langevin description, we write down a generalization of the Heisenberg equations that include damping terms and fluctuating quantum Langevin forces. These equations describe the interaction of the system with a quantum reservoir of a specific sort. For quantum Markov processes, this description is in fact equivalent to a description based on the master equation [5].

For instance, the master equation given as Eq. (2.1) in Ref. [1] is equivalent to the following set of Langevin equations. For the cavity mode, we write

$$\dot{a}=-\Gamma a+H_a+F(t) , \tag{2.1}$$

where H_a denotes the usual Hamiltonian part, and according to the quantum fluctuation-dissipation theorem, the quantum white-noise operator $F(t)$ fulfills the condition

$$[F(t),F^{\dagger}(t')]=2\Gamma\delta(t-t') . \tag{2.2}$$

The master equation of Ref. [1] (or its analog derived with the help of the effective Hamiltonian $\mathcal{H}_{\text{eff}}$ of Ref. [1], (Sec. V) describes the evolution of the reduced density matrix averaged over the noise degrees of freedom. Such an average is evaluated under the assumption that the reservoir is in the vacuum state $|\text{vac}\rangle$, i.e.,

$$F(t)|\text{vac}\rangle=0 . \tag{2.3}$$

Similarly, the atomic Langevin equations in the bare-state description are

$$\begin{aligned}
\dot{\sigma}_\mu&=-\gamma\sigma_\mu+H_{\sigma_\mu}+i\sigma_{3\mu}F_\mu ,\\
\dot{\sigma}_\mu^{\dagger}&=-\gamma\sigma_\mu^{\dagger}+H_{\sigma_\mu^{\dagger}}-iF_\mu^{\dagger}\sigma_{3\mu} ,\\
\dot{\sigma}_{3\mu}&=-2\gamma(\sigma_{3\mu}+1)+H_{\sigma_{3\mu}}+2i(F_\mu^{\dagger}\sigma_\mu-\sigma_\mu^{\dagger}F_\mu) ,
\end{aligned} \tag{2.4}$$

where $H_{\sigma_\mu},H_{\sigma_{3\mu}}$ denote the Hamiltonian parts, $\sigma_\mu,\sigma_{3\mu}$ denote atomic polarization and inversion operators, 2γ denotes the free-space spontaneous emission rate of the atoms, and

$$[F_\mu(t),F_{\mu'}^{\dagger}(t')]=2\gamma\delta_{\mu\mu'}\delta(t-t') . \tag{2.5}$$

We now transform the above equations to the dressed-state basis, using the unitary transformation, given by expression (2.7) of Ref. [1]. If the Hamiltonian part is given by $\mathcal{H}_{\text{eff}}$ (Eq. (5.5) in Ref. [1]), it is convenient to introduce the macroscopic polarization and inversion operators

$$\begin{aligned}
S&=e^{2i\Delta_L t}\sum_\mu e^{-2i\varphi_\mu}\sigma_\mu ,\\
S^{\dagger}&=e^{-2i\Delta_L t}\sum_\mu e^{2i\varphi_\mu}\sigma_\mu^{\dagger} ,\\
S_3&=\sum_\mu \sigma_{3\mu} ,
\end{aligned} \tag{2.6}$$

where Δ_L is to be determined from the "frequency-pulling formula" (Eq. (6.2) in Ref. [1]), and the φ_μ are phases of the atom-cavity mode couplings g_μ entering Eq. (2.2) in Ref. [1]. Note that, according to the theory of Ref. [1] in the stationary limit, the operators $\tilde{S}=\sum_\mu\exp(-2i\varphi_\mu)\sigma_\mu$ and $\tilde{S}^{\dagger}=\sum_\mu\exp(2i\varphi_\mu)\sigma_\mu^{\dagger}$ behave as $\exp(-2i\Delta_L t)\times\text{const}$ and $\exp(2i\Delta_L t)\times\text{const}$, respectively. We have included oscillating factors in Eq. (2.6) to cancel the asymptotic oscillatory behavior of $\tilde{S}$ and $\tilde{S}^{\dagger}$ above threshold so that the operators S and $S^{\dagger}$ are slowly varying in the long-time limit. After some algebra we obtain Langevin-Bloch equations for the macroscopic operators defined in Eq. (2.6):

$$\dot{S}=-[\gamma_1+i(\Omega'-2\Delta_L)]S-i\Lambda_1 S_3 a^2-2i\Lambda_2\left[a^\dagger a+\frac{1}{2}\right]S-\frac{i}{2}e^{2i\Delta_L t}(1+c)\sum_\mu e^{-2i\varphi_\mu}\sigma_{3\mu}F_\mu$$
$$-\frac{i}{2}(1-c)e^{2i\Delta_L t}\sum_\mu e^{-2i\varphi_\mu}F_\mu^\dagger\sigma_{3\mu}-ise^{2i\Delta_L t}\left[\sum_\mu(e^{-2i\varphi_\mu}\sigma_\mu F_\mu+e^{-2i\varphi_\mu}F_\mu^\dagger\sigma_\mu)\right],$$

$$\dot{S}^\dagger=-[\gamma_1-i(\Omega'-2\Delta_L)]S^\dagger+i\Lambda_1(a^\dagger)^2S_3+2i\Lambda_2 S^\dagger\left[a^\dagger a+\frac{1}{2}\right]+\frac{i}{2}(1+c)e^{-2i\Delta_L t}\sum_\mu E^{2i\varphi_\mu}F_\mu^\dagger\sigma_{3\mu}$$
$$+\frac{i}{2}(1-c)e^{-2i\Delta_L t}\sum_\mu e^{2i\varphi_\mu}\sigma_{3\mu}F_\mu+ise^{-2i\Delta_L t}\left[\sum_\mu e^{2i\varphi_\mu}F_\mu^\dagger\sigma_\mu^\dagger+e^{2i\varphi_\mu}\sigma_\mu^\dagger F_\mu\right],$$

$$\dot{S}_3=-\gamma_2(S_e-\bar{S}_3)+2i\Lambda_1[S^\dagger a^2-(a^\dagger)^2S]-i(1+c)\left[\sum_\mu\sigma_\mu^\dagger F_\mu-\sum_\mu F_\mu^\dagger\sigma_\mu\right]+i(1-c)\left[\sum_\mu\sigma_\mu^\dagger F_\mu^\dagger-\sum_\mu\sigma_\mu F_\mu\right],$$

$$\dot{a}=-[\Gamma+i(\Delta_2-\Delta_L)]a+2i\Lambda_1 a^\dagger S-i\Lambda_2 S_3 a+F\ , \tag{2.7a}$$
$$\dot{a}^\dagger=-[\Gamma-i(\Delta_2-\Delta_L)]a^\dagger-2i\Lambda_1 S^\dagger a+i\Lambda_2 a^\dagger S_3+F^\dagger\ , \tag{2.7b}$$

where for conciseness we have used

$$s=\sin 2\alpha$$

and

$$c=\cos 2\alpha\ .$$

The relaxation rate γ_1 (γ_2) is defined in Eq. (3.5) [Eq. (3.6)] of Ref. [1], Λ_1 (Λ_2) is defined in Eq. (5.6a), [Eq. (5.6b)], and $\Delta_L=\omega_{\rm DSL}-\omega_L$, where $\omega_{\rm DSL}$ is the frequency at which the dressed-state laser oscillates. Our aim will be to find the lowest-order corrections to the semiclassical solutions of Eqs. (2.7). (See Sec. V of Ref. [1].) In this way we can describe the leading quantum effects in the case when the number of atoms in the cavity, N, is large. We shall therefore treat the noise terms on the right-hand of Eqs. (2.7) as small perturbations and look for the lowest-order contribution that they give in the stationary limit. Note that this linearization assumption is equivalent to the assumption of Gaussian quasiprobability distributions that describe fluctuations of the system around its stationary state. Such an assumption is commonly used in quantum optics and gives asymtotically exact results far from threshold and in the limit of large N.

It is useful to define the macroscopic noise terms

$$F_1=e^{+2i\Delta_L t}\sum_\mu e^{-2i\varphi_\mu}\sigma_{3\mu}F_\mu\ ,$$
$$F_2=e^{-2i\Delta_L t}\sum_\mu e^{+2i\varphi_\mu}\sigma_{3\mu}F_\mu\ ,$$
$$F_3=e^{+2i\Delta_L t}\sum_\mu e^{-2i\varphi_\mu}\sigma_\mu F_\mu\ ,$$
$$F_4=e^{-2i\Delta_L t}\sum_\mu e^{+2i\varphi_\mu}\sigma_\mu^\dagger F_\mu\ , \tag{2.8}$$
$$F_5=\sum_\mu\sigma_\mu F_\mu\ ,$$
$$F_6=\sum_\mu\sigma_\mu^\dagger F_\mu\ ,$$

and similarly the noise terms $F_i^\dagger$, $i=1,\ldots,6$. The quantum correlation functions of the noise terms (2.8) and their conjugates can be evaluated using the relations (2.5). In order to study the role of quantum fluctuations in the stationary limit, one has to linearize the solutions of Eqs. (2.7) around the stationary semiclassical solutions. With this objective in mind, we shall look for solutions of Eqs. (2.7) having the form

$$\hat{S}=S+\delta\hat{S}\ ,$$
$$\hat{S}_3=S_3+\delta\hat{S}_3\ , \tag{2.9}$$
$$\hat{a}=a+\delta\hat{a}\ ,$$

etc. The caret in Eqs. (2.9) indicates the operator character of the solutions. S, S^*, S_3, a, and a^* denote classical c-number stationary values. The terms that describe quantum corrections, $\delta\hat{S}$, $\delta\hat{S}_3$, $\delta\hat{a}$, etc., are linear functions of the noise terms defined in Eq. (2.8). It is convenient to introduce the radial coordinates

$$a=re^{-i\varphi}\ ,$$
$$S=pe^{-i\psi}\ ,$$

where φ,ψ are real, while r and p denote moduli of a and S, respectively. Analogously, for the quantum parts of expressions (2.9),

$$\delta\hat{a}=(\delta\hat{r}-ir\delta\hat{\varphi})e^{-i\varphi}\ ,$$
$$\delta\hat{S}=(\delta\hat{p}-ip\delta\hat{\psi})e^{-i\psi}\ , \tag{2.10}$$

where $\delta\hat{r}$, $\delta\hat{\varphi}$, $\delta\hat{p}$, and $\delta\hat{\psi}$ are now Hermitian operators.

For reasons that will become clear below, it is useful to introduce the following combinations of quantum phases:

$$\delta\hat{\theta}=\frac{\delta\hat{\varphi}}{2}-\frac{\delta\hat{\psi}}{4}\quad\delta\hat{\phi}=\frac{\delta\hat{\varphi}}{2}+\frac{\delta\hat{\psi}}{4}\ . \tag{2.11}$$

We may now introduce a vector notation and denote the

vector of quantum corrections as

$$\mathbf{x}=(\delta\hat{r},\delta\hat{p},\delta\hat{S}_3,\delta\hat{\theta},\delta\hat{\phi}) \ . \tag{2.12}$$

It is useful to arrange the noise terms into the form of a 14-dimensional vector. Since we work with real and Hermitian variables as in Eqs. (2.10) and (2.11), we shall also introduce real and imaginary parts of the noise terms $F,F^\dagger$:

$$\begin{aligned} F_{0r}&=\frac{Fe^{i\varphi}+F^\dagger e^{-i\varphi}}{2} \ , \\ F_{0i}&=\frac{Fe^{i\varphi}-F^\dagger e^{-i\varphi}}{2i} \ . \end{aligned} \tag{2.13}$$

Similarly, for the noise terms given by Eq. (2.8), we define

$$\begin{aligned} F_{1r}&=\frac{F_1e^{i\psi}+F_1^te^{-i\psi}}{2} \ , \\ F_{2r}&=\frac{F_2e^{-i\psi}+F_2^\dagger e^{i\psi}}{2} \ , \\ F_{3r}&=\frac{F_3e^{i\psi}+F_3^\dagger e^{-i\psi}}{2} \ , \\ F_{4r}&=\frac{F_4e^{-i\psi}+F_4^\dagger e^{-i\psi}}{2} \ , \\ F_{5r}&=\frac{F_5+F_5^\dagger}{2} \ , \\ F_{6r}&=\frac{F_6+F_6^\dagger}{2} \ , \end{aligned} \tag{2.14}$$

with analogous expressions for the imaginary parts. All of the operators in Eqs. (2.13) and (2.14) are Hermitian, and their correlations are related simply to those of F_ν and $F_\nu^\dagger$. For instance, if we arrange the correlations in a matrix form, we obtain

$$\begin{bmatrix} \langle F_{\nu r}(t)F_{\nu' r}(t')\rangle & \langle F_{\nu r}(t)F_{\nu' i}(t')\rangle \\ \langle F_{\nu i}(t)F_{\nu' r}(t')\rangle & \langle F_{\nu i}(t)F_{\nu' i}(t')\rangle \end{bmatrix} = \tfrac{1}{4}\langle F_\nu(t)F_{\nu'}(t')\rangle \begin{bmatrix} 1 & i \\ -i & 1 \end{bmatrix} . \tag{2.15}$$

Let us now define a vector

$$\mathbf{F}=(F_{0r},F_{0i},F_{1r},F_{1i},\ldots,F_{6r},F_{6i}) \ . \tag{2.16}$$

Using the vector notation of Eqs. (2.12) and (2.16), the linearized Langevin-Bloch equations take the form

$$\dot{\mathbf{x}}(t)=\tilde{\mathcal{M}}\mathbf{x}(t)+\tilde{\mathcal{G}}\mathbf{F}(t) \ , \tag{2.17}$$

where $\tilde{\mathcal{M}}$ is a 5×5 matrix that governs the linear stability of the semiclassical stationary solutions, while $\tilde{\mathcal{G}}$ is a 5×14 matrix. Explicit forms of these matrices are given in the Appendixes.

III. PHASE DIFFUSION

We now briefly discuss the properties of the matrix $\tilde{\mathcal{M}}$, leaving a more detailed discussion to Appendix A. First of all, by direct inspection of the semiclassical solutions given in Sec. V of Ref. [1], we observe that the phase $\phi=\varphi/2+\psi/4$ is indeterminate. This fact has the obvious physical meaning that spontaneously generated laser radiation does not have a fixed phase and implies that one of the eigenvalues of the linear stability matrix $\tilde{\mathcal{M}}$ is zero. In fact, for our choice of variables [see Eq. (2.10)] it is the eigenvalue corresponding to the fifth coordinate, $\delta\hat{\phi}$ (see also Appendix A). We can thus write

$$\delta\hat{\phi}(t)=\int_0^t e^{\lambda_j(t-t')}O_5^j(\bar{O}\,{}_k^j)^*G_{k\nu}F_\nu(t')dt' \ . \tag{3.1}$$

In the above expression, a summation convention is used; i.e., all repeated indices j,k,ν are assumed summed. O_k^j and $\bar{O}\,{}_k^j$ denote, respectively, the coordinates of the left and right eigenvectors of the matrix $\tilde{\mathcal{M}}$ corresponding to the eigenvalue λ^j. It is useful to represent the phase $\delta\hat{\phi}(t)$ as a sum of diffusive and nondiffusive parts, $\delta\hat{\phi}(t)=\delta\hat{\phi}_{\rm d}(t)+\delta\hat{\phi}_{\rm nd}(t)$, where $\delta\hat{\phi}_{\rm d}(t)=\int_0^t(\bar{O}\,{}_k^5)^*G_{k\nu}F_\nu(t')dt'$ is the contribution to the right-hand side of Eq. (3.1) that comes from $j=5$ only, and $\delta\hat{\phi}_{\rm nd}(t)$ is the contribution from $j=1,2,3,4$. Because of the fact that $\lambda_5=0$ (see Appendix A), it is easy to show that the correlation function of $\delta\hat{\phi}_{\rm d}$ is a linear function of time and leads to secular divergences in the power spectrum or squeezing spectrum. Therefore, we must treat phase diffusion nonperturbatively.

That is easily accomplished when we take advantage of the fact that we are interested only in the lowest-order corrections to the semiclassical results. Up to linear terms in fluctuations, we may assume that $\delta\hat{\phi}_{\rm d}$ commutes with all of the other fluctuation operators $\delta\hat{r}$, $\delta\hat{\theta}$, $\delta\hat{\phi}_{\rm nd}$, $\delta\hat{p}$, and $\delta\hat{S}_3$. In the long-time limit, we can thus write

$$\begin{aligned} a(t)&=(r+\delta\hat{r})e^{-i(\varphi+\delta\hat{\varphi})} \\ &\simeq[r+\delta\hat{r}-ir(\delta\hat{\theta}+\delta\hat{\phi}_{\rm nd})]e^{-i(\varphi+\delta\hat{\phi}_{\rm d})} \ , \end{aligned} \tag{3.2}$$

where the phase $\hat{\phi}_{\rm d}$ is now included in the exponent. It is straightforward, using the definition of $\delta\hat{\phi}_{\rm d}$, to calculate the correlations of exponential functions of the phase $\delta\hat{\phi}_{\rm d}$. In the following we shall use, in particular,

$$\langle e^{i\delta\hat{\phi}_{\rm d}(t+\tau)}e^{-i\delta\hat{\phi}_{\rm d}(t)}\rangle=e^{-\gamma_{\rm ph}\tau} \ , \tag{3.3}$$

where the phase-diffusion constant is

$$\gamma_{\rm ph}=\tfrac{1}{2}(\bar{O}\,{}_k^5)^*(\bar{O}\,{}_{k'}^5)^*G_{k\nu}G_{k\nu'}H_{\nu\nu'} \ , \tag{3.4}$$

and $H_{\nu\nu'}$ denotes the noise correlation matrix and is defined so as to satisfy

$$\langle F_\nu(t)F_{\nu'}(t')\rangle=H_{\nu\nu'}\delta(t-t') \ ,$$

and which is explicitly given in Appendix B. Similarly,

$$\langle e^{i\delta\hat{\phi}_{\rm d}(t+\tau)}e^{i\delta\hat{\phi}_{\rm d}(t)}\rangle=e^{-\gamma_{\rm ph}(\tau+4t)} \ . \tag{3.5}$$

The expressions (3.3) and (3.5) can be easily derived using the fact that $\delta\hat{\phi}_{\rm d}$ is an integral or, in other words, a sum of δ-correlated and commuting contributions coming from $F_\nu(t)$ at different times. The vacuum state of the reservoir [Eq. (2.3)] is really a tensor product of vacuum states corresponding to each of $F_\nu(t)$ at different times.

Quantum averages in Eqs. (3.3) and (3.5) reduce therefore to the products over all times t of quantum averages of the terms that are exponentials of linear forms of $F_\nu(t)$.

For the parameters we considered in Ref. [1], the phase-diffusion constant is typically of the order of $10^{-4}\gamma_{\rm char}$, where $\gamma_{\rm char}$ is a number on the order of all the other eigenvalues of the matrix $\tilde{\mathcal{M}}$. The phase diffusion process thus happens on a much slower and well-separated time scale from all other processes in the laser—provided we are not too close to threshold. This fact provides yet another support for Eq. (3.2). In writing (3.2) we have neglected the terms of the relative order $\langle[\delta\hat{\phi}_{\rm d},\delta\hat{\phi}_{\rm nd}]\rangle/\langle\delta\hat{\phi}^2_{\rm and}\rangle$ and $\langle[\delta\hat{\phi}_{\rm d},\delta\hat{\theta}]\rangle/\langle\delta\hat{\theta}^2\rangle$. A numerical analysis shows such terms are typically of the order of $(\gamma_{\rm ph}/\gamma_{\rm char})^{1/2}$, i.e., very small.

In the next section, we shall see what influence this fact has on the squeezing spectra.

IV. SQUEEZING SPECTRUM

Our aim in this section will be to derive expressions for the squeezing spectra of dressed-state lasers. In the standard approach, the squeezing spectrum of a specific quadrature component of the laser field is defined by the formula [13].

$$S(\omega,\varphi_q)=\lim_{t\to\infty}2\Gamma\int_{-\infty}^{+\infty}d\tau\, e^{-i\omega\tau}\langle\mathcal{T}[\delta\hat{a}(t+\tau)e^{i\varphi_q}+\delta\hat{a}^\dagger(t+\tau)e^{-i\varphi_q}][\hat{\delta}(t)e^{i\varphi_q}+\delta\hat{a}^\dagger(t)e^{-i\varphi_q}]\rangle\ , \tag{4.1}$$

where the ordering of the operators denoted by $\mathcal{T}$ corresponds to normal ordering of the creation and annihilation parts and apex time ordering [6]. In the formula above, φ_q is the quadrature angle, which characterizes the specific quadrature component of the laser field.

Let us begin our discussion, however, by looking at the power spectrum of the laser, which contributes partially to expression (4.1). The power spectrum of the laser is a Fourier transform of the laser-mode stationary correlation function

$$C(\tau)=\lim_{t\to\infty}\langle a^\dagger(t+\tau)a(t)\rangle\ .$$

The evaluation of $C(\tau)$ proceeds as follows. First, we represent $a^\dagger(t+\tau)$ and $a(t)$ according to Eq. (3.2). Then we shift the exponents containing $\delta\hat{\phi}_{\rm d}$ to the right. Finally, we perform a decorrelation approximation and calculate quantum averages separately for the diffusive and nondiffusive parts of the correlation function. This can be done for the same reasons as discussed in the previous section. It is easy to show that in this case, according to Eq. (3.3),

$$C(\tau)=\left[\lim_{t\to\infty}\langle\{r+\delta\hat{r}(t+\tau)+ir[\delta\hat{\varphi}(t+\tau)+\delta\hat{\phi}_{\rm nd}(t+\tau)]\}\{r+\delta\hat{r}(t)-ir[\delta\hat{\theta}(t)+\delta\hat{\phi}_{\rm nd}(t)]\}\rangle\right]e^{-\gamma_{\rm ph}\tau}\ . \tag{4.2}$$

Obviously, phase diffusion leads to a broadening of all the specific structures in the spectrum by an amount $\gamma_{\rm ph}$. When $\gamma_{\rm ph}$ is much smaller than all the other widths in the problem (which is indeed the case), the effects of $\gamma_{\rm ph}$ may be safely neglected by letting $\gamma_{\rm ph}=0$ in Eq. (4.2).

When one calculates the squeezing spectrum $S(\omega,\varphi_q)$, one must also evaluate linear combinations of the Fourier transforms of the correlation functions such as

$$D(t,\tau)=\langle a(t+\tau)a(t)\rangle\ .$$

According to Eq. (3.5), such correlations behave differently:

$$D(t,\tau)=\left[\lim_{t\to\infty}\langle\{r+\delta\hat{r}(t+\tau)-ir[\delta\theta(t+\tau)+\delta\hat{\phi}_{\rm nd}(t+\tau)]\}\{r+\delta\hat{r}(t)-ir[\delta\hat{\theta}(t)+\delta\hat{\phi}_{\rm nd}(t)]\}\rangle\right]e^{-\gamma_{\rm ph}(4t+\tau)}\ . \tag{4.3}$$

As we see from Eq. (4.3), the correlation $D(t,\tau)$ tends to zero as $t\to\infty$; thus the squeezing spectrum becomes proportional to the power spectrum of the laser radiation and takes only positive values.

There are, however, in principle at least three methods to avoid the coherence destroying effect of phase diffusion.

(a) Transient squeezing spectrum. First of all, since $\gamma_{\rm ph}$ is much smaller than all the other characteristic widths in the problem ($\gamma_{\rm char}$), we may limit ourselves to finite-time detection. In principle, we should then use the theory of Ref. [15], but let us additionally assume that

$$\gamma_{\rm ph}\ll\frac{1}{\tau_{\rm obs}}\ll\gamma_{\rm char}\ , \tag{4.4}$$

where $\tau_{\rm obs}$ is the observation time. In such a case, we may calculate the transient squeezing spectrum assuming the stationary limit with respect to the time scales $1/\gamma_{\rm char}$ and neglect $\gamma_{\rm ph}$ completely. Such a quantity may be measured in the standard homodyne or heterodyne scheme [18]. In other words, we will then express the spectrum through the correlations

$$C_{ij}(t,\tau)=\langle\delta x_i(t+\tau)\delta x_j(t)\rangle\ ,$$

and in evaluation of $C_{ij}(t,\tau)$, we will neglect the contributions from the fifth eigenvector of the matrix $\tilde{\mathcal{M}}$ completely. It is easy to check that such correlations have a well-defined stationary limit and vanish for $\tau\to\infty$. Using the notation of Appendixes A and B, we obtain

$$\langle \delta x_i(t+\tau)\delta x_j(t)\rangle = \int_0^{t+\tau}\int_0^t e^{\lambda_{j'}(t+\tau-t')+\lambda_{j''}(t-t'')} \times O_i^{j'}O_j^{j''}(\bar{O}_k^{j'})^*(\bar{O}_{k'}^{j''})^* \times G_{kv}G_{k'v'}H_{vv'}\delta(t'-t'')dt'\,dt'' . \quad (4.5)$$

In the above formula the summation over all (at least twice) repeated indices is performed. The summation over j' and j'', however, runs from 1 to 4 only.

Introducing the diffusion matrix

$$D_{jj'}=(\bar{O}_k^j)^*(\bar{O}_{k'}^{j'})^*G_{kv}G_{k'v'}H_{vv'} , \quad (4.6)$$

we easily see that, for $t\to\infty$,

$$\langle \delta x_g(t+\tau)\delta x_h(t)\rangle = -\frac{e^{\lambda_j\tau}}{\lambda_j+\lambda_{j'}}O_h^jO_g^{j'}D_{j'j} . \quad (4.7)$$

(b) Injected signal and phase locking. The second method of dealing with the phase diffusion is to lock the phase. That can be done, for instance, by injecting a signal into the laser cavity. Since the switching on of the two-photon laser requires the injection of a seed field anyway, phase locking is natural in this case. For sufficiently weak injection signals, we expect that the squeezing spectrum of the laser will remain the transient squeezing spectrum, calculated according to the prescription discussed in point (a).

(c) Self-homodyne scheme. Detection of squeezing is often accomplished with the help of a homodyne scheme [18] in which the signal to be measured is mixed with the strong signal of the local oscillator. We may, however, homodyne the laser radiation with itself, so that the diffusion phase will simply cancel from the correlation functions. The measurement of the intensity-intensity correlation function in the limit of a strong laser signal reduces then to the measurement of the variance of some quadrature of the laser field. However, in this type of measurement scheme, it is hard to optimize the spectrum with respect to quadrature angle φ_q [see Eq. (4.1)].

We shall focus our attention in this paper on two quantities that may be measured within scheme (a), (b), or (c). We shall discuss the squeezing spectrum $S(\omega)$, which is defined as the spectrum optimized with respect to the quadrature angle φ_q (see Ref. [14]), i.e.,

$$S(\omega)=\min_{\varphi_q}S(\omega,\varphi_q)=4\Gamma\int_0^\infty\cos(\omega t)[\langle a^\dagger(t+\tau)a(t)\rangle+\langle a^\dagger(t)a(t+\tau)\rangle]-8\Gamma\left|\int_0^\infty\cos(\omega t)\langle a(t+\tau)a(t)\rangle\right| . \quad (4.8)$$

Using the notation introduced above and in Appendixes A and B and neglecting the effect of phase diffusion, we may write down

$$S(\omega)=4\Gamma\frac{\lambda_j}{(\lambda_j^2+\omega^2)}\frac{1}{(\lambda_j+\lambda_{j'})}\{D_{jj'}[O_1^jO_1^{j'}+r^2O_{\rm ph}^jO_{\rm ph}^{j'}+ir(O_{\rm ph}^jO_1^{j'}-O_1^jO_{\rm ph}^{j'})]\} +D_{j'j}[O_1^jO_1^{j'}+r^2O_{\rm ph}^jO_{\rm ph}^{j'}+ir(O_1^jO_{\rm ph}^{j'}-O_{\rm ph}^jO_1^{j'})] -8\Gamma\left|\frac{\lambda_j}{(\lambda_j^2+\omega^2)}\frac{1}{(\lambda_j+\lambda_{j'})}D_{jj'}[O_1^jO_1^{j'}-r^2O_{\rm ph}^jO_{\rm ph}^{j'}-ir(O_{\rm ph}^jO_1^{j'}+O_1^jO_{\rm ph}^{j'})]\right| , \quad (4.9)$$

where the "phase" component of the eigenvectors is $O_{\rm ph}^j=O_4^j+O_5^j$, and the sums run over J and j' from 1 to 4.

Also, we shall present the results for an optimized squeezing factor $S_{\rm op}$ defined as [14]

$$S_{\rm op}=\min_\omega S(\omega) . \quad (4.10)$$

We shall study the dependence of this quantity on parameters characterizing dressed-state lasers and, in particular, its dependence on the cavity-pump detuning Δ_2.

V. SQUEEZING SPECTRA OF DRESSED-STATE LASERS

In this section we present the results of our numerical analysis of the squeezing spectra for dressed-state lasers Two kinds of graphs are presented. For each set of parameters, we first find the optimized squeezing factor, defined as in Eq. (4.10), as a function of the cavity-pump detuning Δ_2. The optimized squeezing factor is drawn with the direction of the vertical axis reversed so that the maximal squeezing (minimal $S_{\rm op}$) is at the top. Calculations are limited to those values of Δ_2 belonging to the region of laser stability and the region of self-consistency of our theory (see Sec. VI of the preceding paper). Stability boundaries are indicated in the figures by (a) capital S, while self-consistency boundaries by a capital C. We also present examples of the squeezing spectrum $S(\omega)$ calculated for specific values of Δ_2. In these cases the vertical axis is *not* reversed, so that maximal squeezing occurs for minimal $S(\omega)$.

Let us begin our discussion with the one-photon dressed-state laser. We distinguish two parameter regimes with markedly different squeezing behaviors. The two regimes are distinguished on the basis of the size of the atom-cavity coupling constant g relative to other

quantities such as γ. In many standard laser cavities, g/γ is quite small. On the other hand, relatively large g/γ values arise in situations where very small or highly mode degenerate cavities are employed Figure 1 shows the optimized squeezing factor as a function of Δ_2 for a one-photon laser configuration possessing a small g/γ value. Squeezing is only observed close to the stability limits, indicated by the capital S's in the figure, and is rather small. This is consistent with the results of the preceding paper, which show that for such a laser Bloch-Siegert shifts are of practically no importance. In between the two peaks shown in Fig. 1, the laser is stable, but for these values of the laser-pump detuning, squeezing spectra are positive. The insert shows two squeezing spectra calculated for values of Δ_2 within the two squeezing regions. Note that the squeezing spectrum corresponding to the larger value of Δ_2 is negative only very close to $\omega=0$. Such narrow features in the spectrum may be hard to observe in a finite-time measurement (see discussion in Sec. IV).

Figures 2–7 correspond to high-g/γ cavities. As shown in the preceding paper, Bloch-Siegert shifts are very important in such cavities and may therefore lead to laser action that is significantly different from that predicted using the standard one-photon-laser mode [9]. It turns out, as we shall see below, that Bloch-Siegert effects strongly influence the quantum-statistical properties of the emitted laser radiation and, in fact, lead to large squeezing effects that are absent in the standard case. Figure 2 presents the optimized squeezing factor for several values of Ω'. The largest squeezing corresponds to the smallest value of Ω', relating this effect once more to the relevance of the Bloch-Siegert shift, which is of the order of g^2/Ω'. For the same reason, squeezing disappears for sufficiently large Ω'. The optimized squeezing factor typically has two maxima that occur for values of Δ_2 close to the laser stability boundaries.

Figure 3 shows exemplary squeezing spectra for

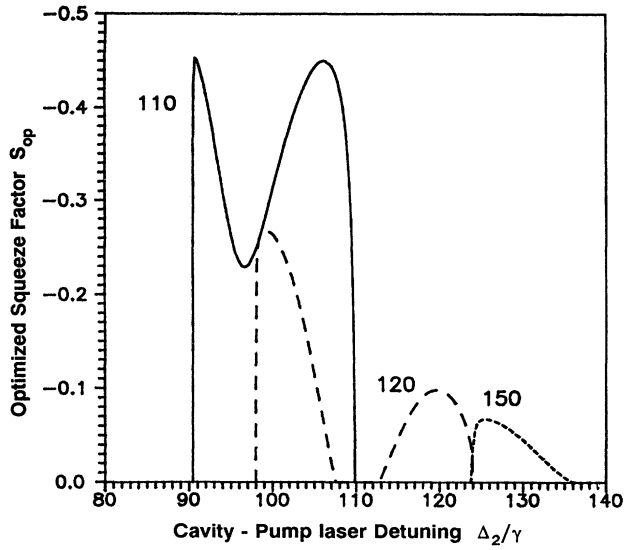

FIG. 2. Optimized squeezing factor S_{op} for the single-photon dressed-state laser as a function of Δ_2. Other parameters are $\Delta_1=-100$, $\Gamma=2.0$, $g=0.5$, and $N=5\times10^4$. The values of Ω' are indicated in the figure. Note that Δ_2 is given in units of γ, i.e., one-half of the spontaneous atomic emission rate.

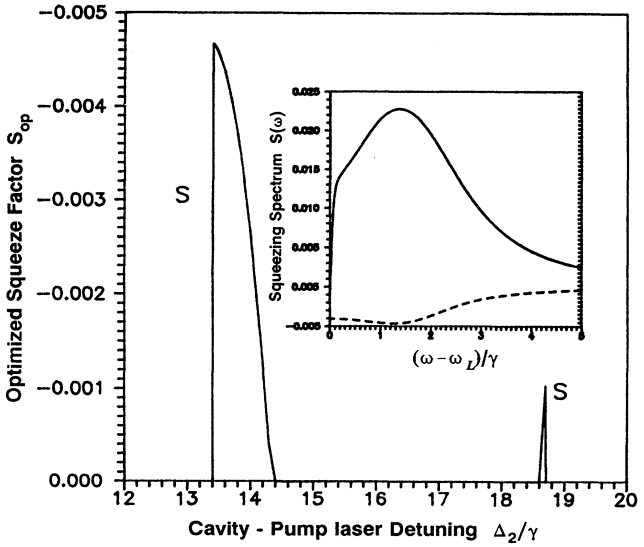

FIG. 1. Optimized squeezing factor S_{op} for the single-photon dressed-state laser as a function of Δ_2. Other parameters are $\Omega'=16$, $\Delta_1=-12$, $\Gamma=0.1$, $g=0.01$, and $N=10^6$. In the insert we show squeezing spectra $S(\omega)$ for two values of $\Delta_2=13.45$ (dashed line) and $\Delta_2=18.7$ (solid line). Note that Δ_2 and $\omega-\omega_L$ are given in units of γ, i.e., one-half of the spontaneous atomic emission rate.

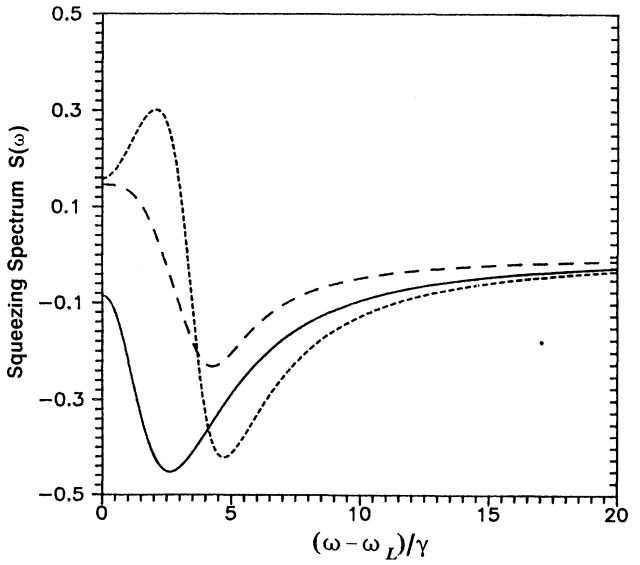

FIG. 3. Examples of squeezing spectrum $S(\omega)$ for the single-photon dressed-state laser for the parameters of Fig. 2: $\Omega'=110$, $\Delta_1=-100$, $\Gamma=2.0$, $g=0.5$, and $N=5\times10^4$. The values of Δ_2 are 91 (solid line), 97 (long-dashed line), and 108 (short-dashed line). Note that $\omega-\omega_L$ is given in units of γ, i.e., one-half of the spontaneous atomic emission rate.

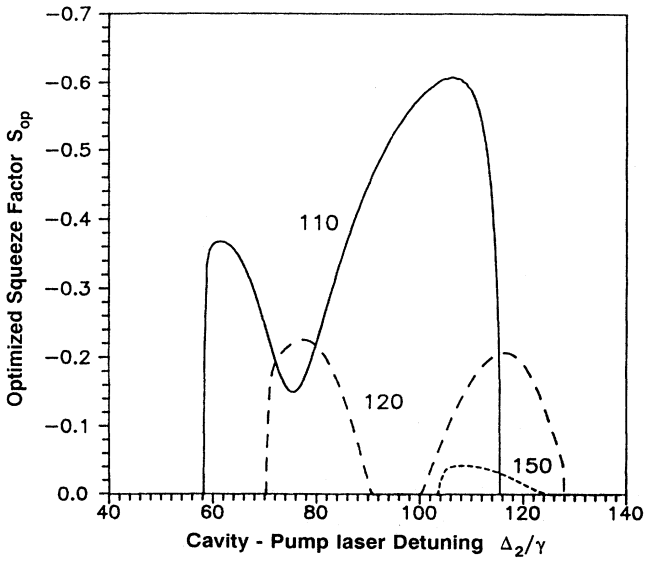

FIG. 4. Optimized squeezing factor S_{op} for the single-photon dressed-state laser as a function of Δ_2. Other parameters are $\Delta_1=-100$, $\Gamma=2.0$, $g=0.5$, and $N=10^5$. The values of Ω' are indicated in the figure. Note that Δ_2 is given in units of γ, i.e., one-half of the spontaneous atomic emission rate.

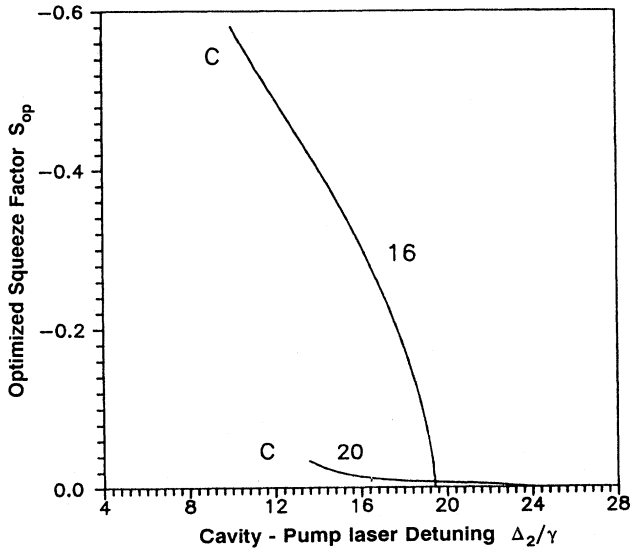

FIG. 6. Optimized squeezing factor S_{op} for the single-photon dressed-state laser as a function of Δ_2. Note the Δ_2 is given in units of γ, i.e., one-half of the spontaneous atomic emission rate. Other parameters are $\Delta_1=-12$, $\Gamma=2.0$, $g=0.2$, and $N=10^5$. The values of Ω' are indicated in the figure.

different values of Δ_2. The frequency of maximal squeezing increases with increasing cavity-pump detuning Δ_2. Figures 4 and 5 are drawn for a larger number of atoms N. Note that the optimal squeezing factor increases in this case with N. Figures 6 and 7 correspond to a different choice of parameters and, in particular, to the case of a relatively small atom-pump detuning Δ_1. Note that the optimized squeezing curves differ in this case from the previously discussed case of large Δ_1. First of all, no maximum at the right stability boundary is observed. The curves are limited this time by the consistency condition [Eq. (6.11) of Ref.[1]]. The region in which

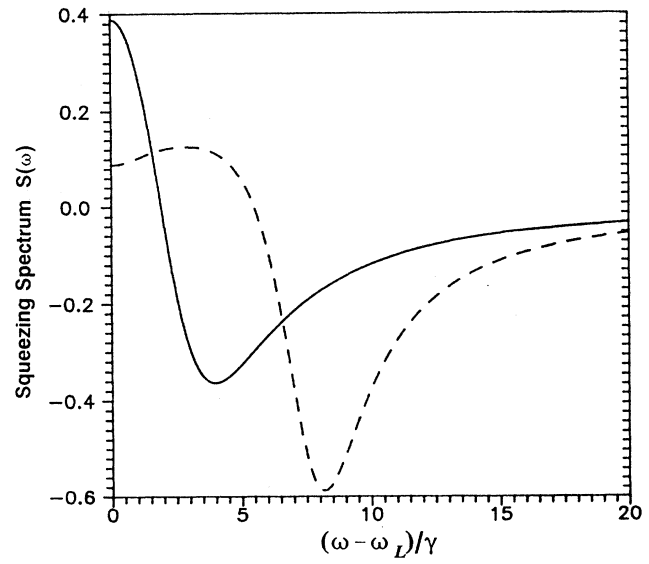

FIG. 5. Examples of squeezing spectrum $S(\omega)$ for the single-photon dressed-state laser for the parameters of Fig. 4: $\Omega'=110$, $\Delta_1=-100$, $\Gamma=2.0$, $g=0.5$, and $N=5\times10^4$. The values of Δ_2 are 60 (solid line) and 110 (dashed line). Note that $\omega-\omega_L$ is given in units of γ, i.e., one-half of the spontaneous atomic emission rate.

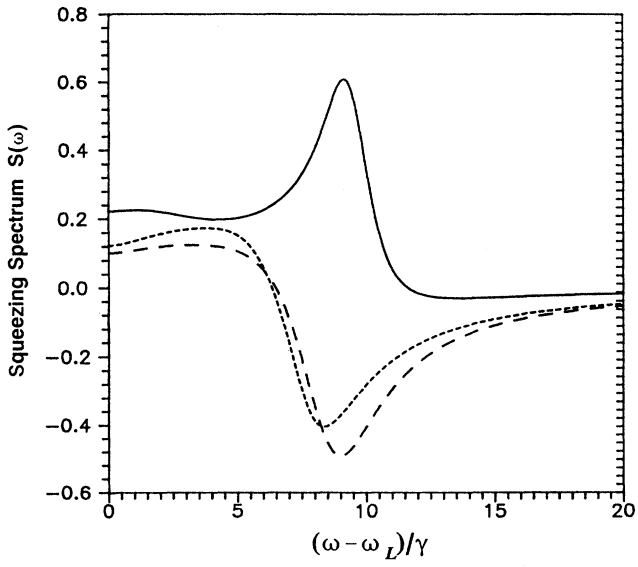

FIG. 7. Examples of squeezing spectrum $S(\omega)$ for the single-photon dressed-state laser for the parameters of Fig. 5: $\Delta_1=-12$, $\Gamma=2.0$, $g=0.2$, and $N=10^5$. The values of Ω' and Δ_2 are 20 and 14 (solid line), 16 and 12 (long-dashed line), and 16 and 14 (short-dashed line). Note that $\omega-\omega_L$ is given in units of γ, i.e., one-half of the spontaneous atomic emission rate.

the consistency condition is important is indicated in Fig. 6 by the capital C's. The spectra in Fig. 7 exhibit complex behavior (shifts of the maximal squeezing frequency, qualitative shape changes) as a function of Ω' and Δ_2.

We may summarize the results for the one-photon dressed-state laser as follows. It is well known that the standard theory of the single-mode laser does not lead to any kind of significant quantum effects and that the quantum state of the laser light may be very well approximated by a coherent state [6]. Our theory differs from the standard one by the presence of the Bloch-Siegert type of terms. Contrary to the standard Bloch-Siegert shifts, which are, of course, negligible in the optical domain [4], analogous terms appear in our theory because of the presence of "antiresonant" transitions in the dressed-state description of the system (see Sec. IV, Ref. [1]). The antiresonant transitions in question belong to three groups: (a) transitions between upper-upper or lower-lower dressed states that are accompanied by cavity photon emission or absorption, (b) transitions from the more populated dressed state to the less populated dressed state accompanied by photon absorption, and (c) transitions from the less populated dressed state to the more populated dressed state accompanied by photon emission.

All of these processes compete in a coherent way with standard one-photon transitions in the dressed-state laser, leading to frequency shifts. The Bloch-Siegert dressed-state shifts are typically of the order of g^2/Ω' and, apparently, cannot be neglected in our theory.

Although Bloch-Siegert shifts scarcely affect the stability properties of dressed-state lasers, they play an enormous role in determining statistical properties of laser radiation. It is amazing to see that the antiresonant terms in the dressed-state Hamiltonian (Sec. II, Ref. [1]), which lead to Bloch-Siegert effect, at the same time may lead to large squeezing of the one-photon dressed-state laser. Large squeezing effects are predicted to occur in high-g cavities, in which case Bloch-Siegert effects are typically more pronounced than for low-g cavities.

Our results suggest that the standard low-frequency maser, constructed with a high-g cavity, may serve as a source of bright squeezed radiation. Owing to the smallness of maser resonant frequencies, Bloch-Siegert effects may be relatively large and may be related to squeezing in a manner analogous to that discussed here for the case of the one-photon dressed-state laser.

One should stress also that the inclusion of the Bloch-Siegert shift leads to a theory that is very rich and leads to a whole variety of results that are not easy to interpret. The magnitude of the squeezing effects is quite robust with respect to parameter changes, but the shapes of squeezing spectra and optimized squeezing diagrams vary significantly.

Let us now consider the case of the two-photon dressed-state laser. As before, we discuss first the low-g cavity (see Fig. 8). The squeezing appears only in the vicinity of the stability boundaries, indicated by the capital S's, and is rather small. Note the extremely sharp peak at the right Δ_2 limit. Although the squeezing here is large, it may be hard to observe. Since the squeezing has a very narrow Δ_2 bandwidth, it would require a highly monochromatic and well-stabilized pump laser to avoid a smearing out of this feature.

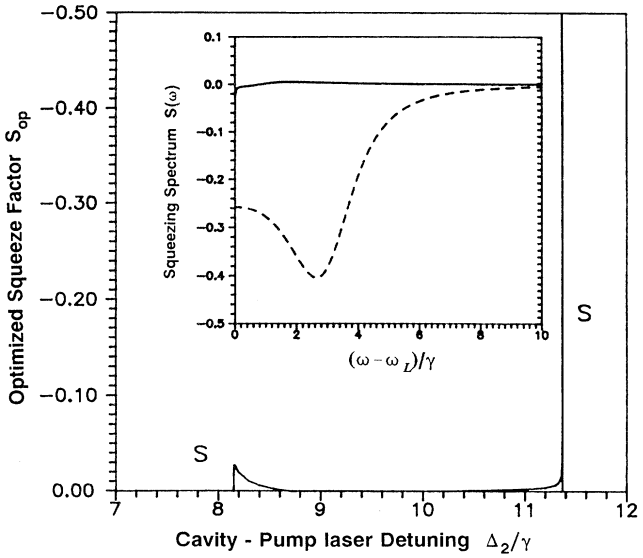

FIG. 8. Optimized squeezing factor S_{op} for the two-photon dressed-state laser as a function of Δ_2. Other parameters are $\Omega'=16$, $\Delta_1=-12$, $\Gamma=0.1$, $g=0.01$, and $N=10^6$. In the insert we show exemplary squeezing spectra $S(\omega)$ for two values of $\Delta_2=11.367\,79$ (dashed line) and $\Delta_2=8.156$ (solid line). Note that Δ_2 and $\omega-\omega_L$ are given in units of γ, i.e., one-half of the spontaneous atomic emission rate.

The insert shows the squeezing spectra for laser-pump detunings corresponding to the left and right peaks in the figure. The squeezing in the spectrum corresponding to the lower value of Δ_2 is narrow band in ω. Therefore, it may not be hard to observe it in the limited-time measurement as discussed above.

Figures 9–16 correspond to the two-photon laser in a high-g cavity. Figures 9–11 correspond to $\Omega'=120$. Figure 9 shows the optimized squeezing factor S_{op} for the values of the cavity width Γ shown. As in the low-g case, squeezing is maximal close to the stability limits (indicated by capital S's). It is also quite large close to the consistency limits (indicated by capital C's). Since squeezing increases when the parameters approach their threshold values, larger Γ leads typically to larger squeezing. This can be understood in the following way: Close to threshold the competition between resonant (Sec. III, Ref. [1]) and antiresonant terms (Sec. IV, Ref. [1]) in the dressed-state Hamiltonian becomes more pronounced. Figure 10 displays the squeezing spectrum for several values of Δ_2 taken from along the solid curve of Fig. 9. Note that the frequency of maximal squeezing jumps abruptly to $\omega=0$ at the largest value of Δ_2. This fact explains the nonanalytic behavior of the solid curve in Fig. 9. Figure 11 shows the squeezing spectra in the vicinity of the stability limit. Critical slowing down and critical fluctuation exhibit themselves in the squeezing spectrum in the form of large positive peaks at frequencies corresponding to the imaginary part of the stability-matrix eigenvalue whose real part tends to zero at the stability limit. Note, howev-

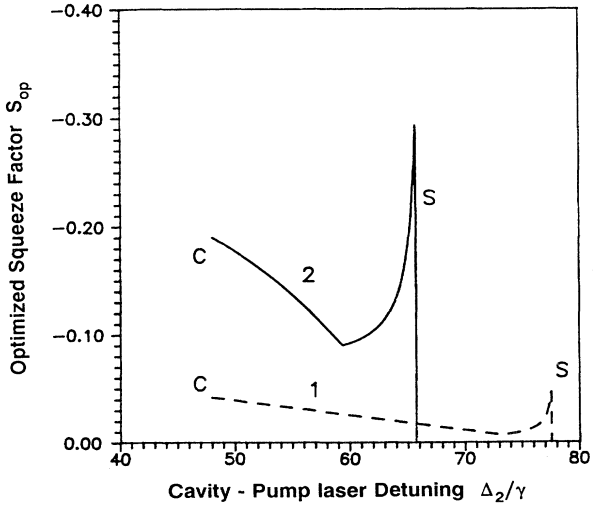

FIG. 9. Optical squeezing factor S_{op} for the two-photon dressed-state laser as a function of Δ_2. Other parameters are $\Delta_1=-100$, $\Omega'=120$, $g=0.5$, and $N=10^5$. The values of Γ are indicated in the figure. Note that Δ_2 is given in units of γ, i.e., one-half of the spontaneous atomic emission rate.

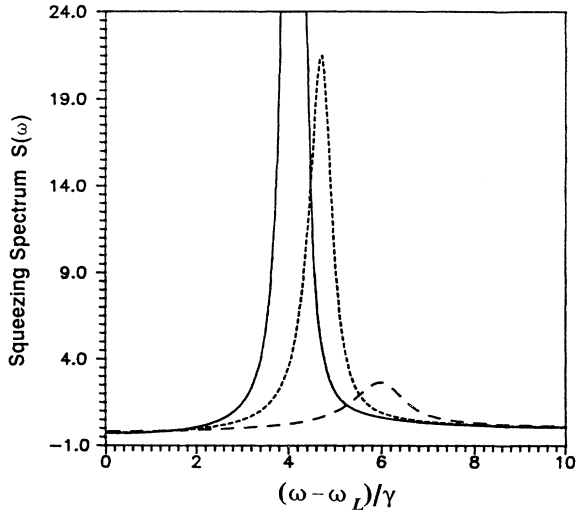

FIG. 11. Examples of squeezing spectrum $S(\omega)$ for the two-photon dressed-state laser for the parameters of Fig. 9: $\Delta_1=-100$, $\Omega'=120$, $\Gamma=2$, $g=0.5$, and $N=10^5$. The values of Δ_2 are 65.66 (solid line), 65.6 (short-dashed line), and 65 (long-dashed line). Note that $\omega-\omega_L$ is given in units of γ, i.e., one-half of the spontaneous atomic emission rate.

er, that the positive peaks that describe large classical fluctuations are surrounded by the broadband regions of negative $S(\omega)$, i.e., reduced, quantum fluctuations. Only in the immediate neighborhood of the stability limit does the squeezing spectrum become totally positive (see the abrupt decrease of S_{op} at the stability border in Fig. 9). Figures 12–14 correspond to the case of a slightly larger value of $\Omega'=140$. The optimized squeezing factor S_{op} is presented in Fig. 12 for three different values of the number of active atoms, N. As above, the capital C's and S's in the figure correspond to parameter limits set by consistency and stability conditions, respectively. Note that large squeezing can be obtained for small values of N, i.e., close to the lasing threshold. Exemplary spectra corresponding to this case ($N=50\,000$) are shown in Fig. 13. Note that the maximal squeezing appears at $\omega=0$, i.e., at

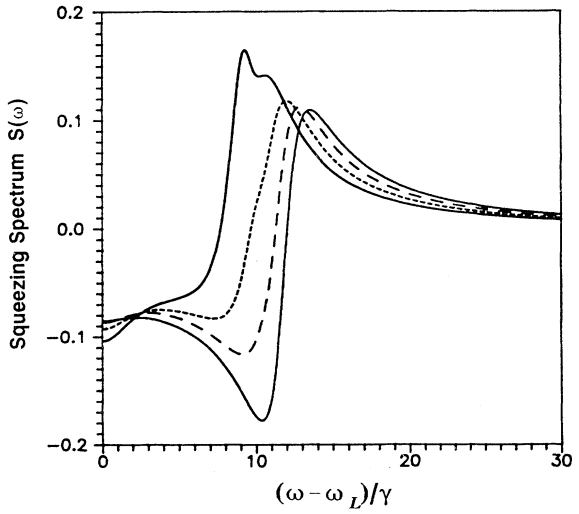

FIG. 10. Examples of squeezing spectrum $S(\omega)$ for the two-photon dressed-state laser for the parameters of Fig. 9: $\Delta_1=-100$, $\Omega'=120$, $\Gamma=2$, $g=0.5$, and $N=10^5$. The values of Δ_2 are 62, 60, 57, and 50 from left to right. Note that $\omega-\omega_L$ is given in units of γ, i.e., one-half of the spontaneous atomic emission rate.

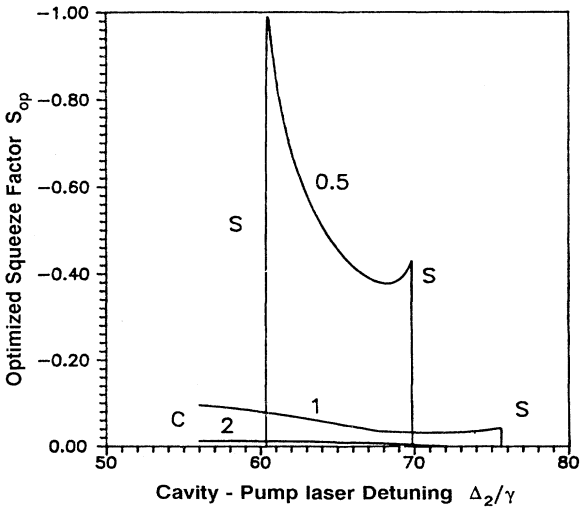

FIG. 12. Optimized squeezing factor S_{op} for the two-photon dressed-state laser as a function of Δ_2. Other parameters are $\Delta_1=-100$m, $\Omega'=140$, $g=0.5$, and $\Gamma=2$. The values of $N/10^5$ are indicated in the figure. Note that Δ_2 is given in units of γ, i.e., one-half of the spontaneous atomic emission rate.

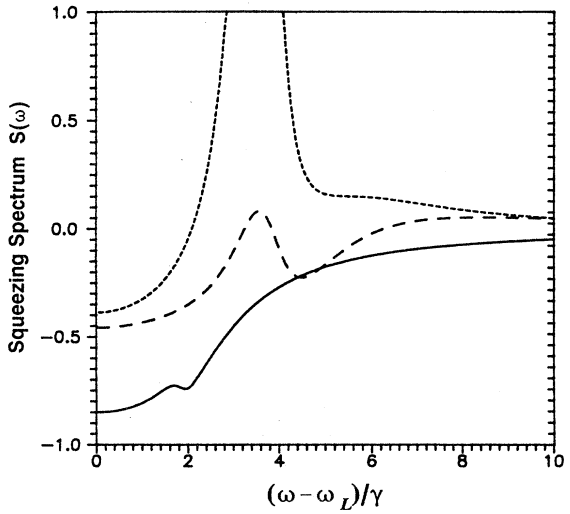

FIG. 13. Examples of squeezing spectrum $S(\omega)$ for the two-photon dressed-state laser for the parameters of Fig. 12: $\Delta_1=-100$, $\Omega'=140$, $\Gamma=2$, $g=0.5$, and $N=5\times10^4$. The values of Δ_2 are 61 (solid line), 65 (long-dashed line), and 69 (short-dashed line). Note that $\omega-\omega_L$ is given i units of γ, i.e.,one-half of the spontaneous atomic emission rate.

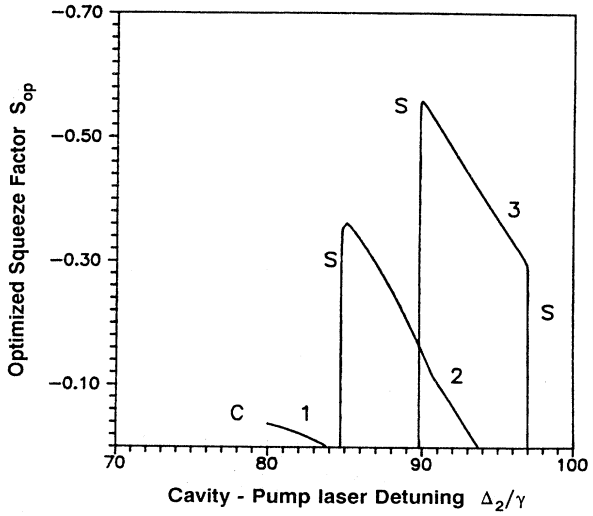

FIG. 15. Optimized squeezing factor S_{op} for the two-photon dressed-state laser as a function of Δ_2. Other parameters are $\Delta_1=-100$, $\Omega'=200$, $g=0.5$, and $N=10^5$. The values of Γ are indicated in the figure. Note that Δ_2 is given in units of γ, i.e., one-half of the spontaneous atomic emission rate.

the lasing frequency. The shape of the squeezing spectrum is quite rich and depends strongly on N, as shown in Fig. 14.

Figure 15 and 16 correspond to yet larger values of Ω'. In Fig. 15 parameter limits set by consistency and stability conditions are indicated by the capital C's and S's, respectively. The behavior of the optimized squeezing factor S_{op} is quite regular in this regime. As before, larger squeezing corresponds to larger cavity width. Squeezing spectra (Fig. 16) show that the squeezing occurs for a broadband of frequencies, but not in the immediate neighborhood of the frequency related to the most relevant eigenvalue of the stability matrix.

Summarizing, we should stress that, as in the case of the one-photon dressed-state laser, significant squeezing may occur for two-photon dressed-state lasers in high-g cavities. On the other hand, squeezing remains on a level of at most a few percent for lasers in low-g cavities. Generally, the squeezing is bigger for values of parameters

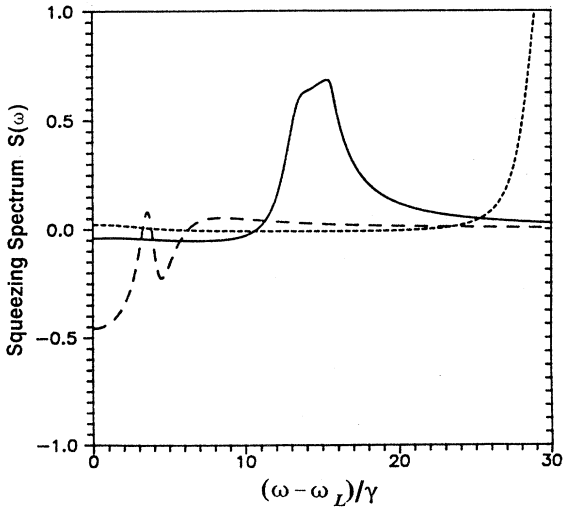

FIG. 14. Examples of squeezing spectrum $S(\omega)$ for the two-photon dressed-state laser for the parameters of Fig. 12: $\Delta_1=-100$, $\Omega'=140$, $\Gamma=2$, $g=0.5$, and $\Delta_2=65$. The values of $N/10^5$ are 1 (solid line), 0.5 (long-dashed line), and 0.2 (short-dashed line). Note that $\omega-\omega_L$ is given in units of γ, i.e., one-half of the spontaneous atomic emission rate.

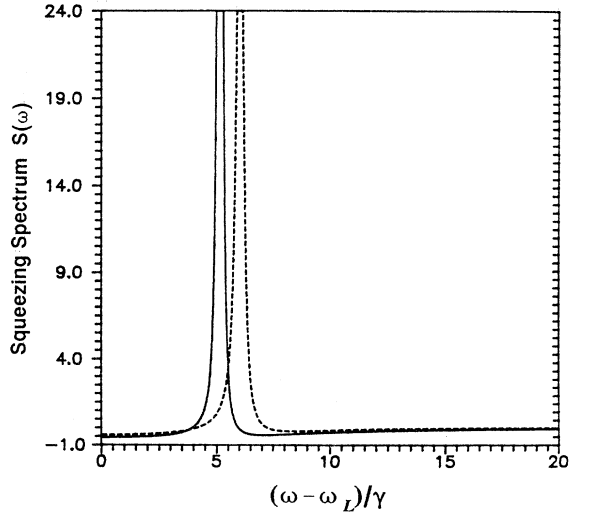

FIG. 16. Examples of squeezing spectrum $S(\omega)$ for the two-photon dressed-state laser for the parameters of Fig. 15: $\Delta_1=-100$, $\Omega'=200$, $\Gamma=3$, $g=0.5$, and $N=5\times10^4$. The values of Δ_2 are 90 (solid line) and 94 (dashed line). Note that $\omega-\omega_L$ is given in units of γ, i.e., one-half of the spontaneous atomic emission rate.

that correspond to the vicinity of the laser threshold (smaller N, larger Γ).

The squeezing for both one- and two-photon dressed-state lasers has a transient character or must be observed in a phase-locked or a self-homodyne scheme, as discussed in Sec. IV. Nevertheless, within these limitations, we conclude this paper by stating that dressed-state lasers could be used for generating bright squeezed light.

Since completion of this work, we have learned of related work by Agarwal [19,20]. He treats only single-photon lasing, works in the lowest-order rotating-wave approximation, and neglects Bloch-Siegert shifts. Using a quasiprobability approach, he finds that one-photon dressed-state lasers possess statistical properties analogous to those of standard lasers. Our results, which are more accurate since they include the Bloch-Siegert shift, indicate that dressed-state lasers may have quite interesting quantum statistical properties. In this respect, theories that neglect Bloch-Siegert shifts cannot be considered complete.

ACKNOWLEDGMENTS

We acknowledge the support of the Polish Government Program, Grant No. CPBP 01.07, for (M.L.) and (J.Z.), and T.W.M. acknowledges financial support from the U.S. National Science Foundation (Grant No. PHY-9103132) and the U.S. Army Research Office (Grant No. DAAL03-91-6-0313).

APPENDIX A

The linearized Langevin equations, as we already stated, have the form

$$\dot{\mathbf{x}}=\mathcal{M}\mathbf{x}+\tilde{\mathcal{G}}\mathbf{F} , \tag{A1}$$

where the matrix $\tilde{\mathcal{M}}$ is the same matrix that governs the linear stability of the semiclassical solutions. The matrix $\tilde{\mathcal{M}}$, a 5×5 matrix, is found to be

$$\tilde{\mathcal{M}}=\begin{bmatrix} 0 & -2\Lambda_1 r\sin4\theta & 0 & 8\Lambda_1 rp\cos4\theta & 0 \\ -2\Lambda_1 S_3 r\sin4\theta & -\gamma_1 & -\Lambda_1 r^2\sin4\theta & -4\Lambda_1 S_3 r^2\cos4\theta & 0 \\ 8\Lambda_1 pr\sin4\theta & 4\Lambda_1 r^2\sin4\theta & -\gamma_2 & 16\Lambda_1 pr^2\cos4\theta & 0 \\ -r\left[\Lambda_2+\dfrac{\Lambda_2 S_3}{2p}\cos4\theta\right] & \Lambda_1\cos(4\theta)\left[\dfrac{S_3 r^2}{4p^2}-1\right] & \dfrac{1}{2}\left[\Lambda_2-\dfrac{\Lambda_1 r^2}{2p}\cos4\theta\right] & 4\Lambda_2 p+\dfrac{\Lambda_1 S_3 r^2}{p}\sin4\theta & 0 \\ r\left[\Lambda_2+\dfrac{\Lambda_1 S_3}{2p}\cos4\theta\right] & \Lambda_1\cos(4\theta)\left[\dfrac{S_3 r^2}{4p^3}+1\right] & \dfrac{1}{2}\left[\Lambda_2+\dfrac{\Lambda_1 r^2}{2p}\cos4\theta\right] & 4\Lambda_2 p-\dfrac{\Lambda_1 S_3 r^2}{p}\sin4\theta & 0 \end{bmatrix} . \tag{A2}$$

The linear stability of the stationary solutions requires that all of the eigenvalues of the matrix $\tilde{\mathcal{M}}$ have negative real parts.

In general, the matrix $\tilde{\mathcal{M}}$ is not symmetric. It has therefore left and right eigenvectors O^j and $\bar{O}^j$:

$$\begin{aligned} &M_{ik}O_k^j=\lambda_j O_i^j , \\ &M_{ki}^*\bar{O}_k^j=\lambda_j^*\bar{O}_i^j , \\ &\tilde{\mathcal{M}}O^j=\lambda_j O^j , \\ &\tilde{\mathcal{M}}^\dagger\bar{O}^j=\lambda_j^*\bar{O}^j , \end{aligned} \tag{A3}$$

where λ^j denote eigenvalues of the matrix $\tilde{\mathcal{M}}$. The eigenvectors O^j and $\bar{O}^j$ can be chosen to be bi-orthonormal, i.e.,

$$(\bar{O}_k^{j'})^*O_k^j=\delta_{jj} . \tag{A4}$$

Note that phase-diffusion effect exhibits itself in the form of the matrix $\tilde{\mathcal{M}}$ that has the fifth column equal to zero. This implies that the fifth right eigenvector is

$$O_k^5=(0,0,0,0,1) .$$

Similarly, left eigenvectors have

$$\bar{O}_5^j=0 ,$$

for $j=1,2,3,4$.

APPENDIX B

The matrix $\tilde{\mathcal{G}}$ of Eq. (2.17) has the form

$$\tilde{\mathcal{G}}=\begin{bmatrix}
1 & 0 & 0 & 0 & 0 & 0 & 0 & 0 & 0 & 0 & 0 & 0 & 0 & 0 \\
0 & 0 & 0 & -\frac{1+c}{2} & 0 & \frac{c-1}{2} & 0 & s & 0 & -s & 0 & 0 & 0 & 0 \\
0 & 0 & 0 & 0 & 0 & 0 & 0 & 0 & 0 & 0 & 0 & 2(1-c) & 0 & 2(1+c) \\
0 & -\frac{1}{2r} & \frac{1+c}{8s} & 0 & \frac{c-1}{8s} & 0 & -s & 0 & -s & 0 & 0 & 0 & 0 & 0 \\
0 & -\frac{1}{2r} & \frac{1+s}{8s} & 0 & \frac{1-c}{8s} & 0 & s & 0 & s & 0 & 0 & 0 & 0 & 0
\end{bmatrix} . \tag{B1}$$

Additionally, we denote by $H_{\nu\nu'}$ a 14×14 noise correlation matrix defined through

$$\langle F_\nu(t)F_{\nu'}(t')\rangle = H_{\nu\nu'}\delta(t-t') , \tag{B2}$$

where

$$\tilde{\mathcal{H}}=\begin{bmatrix}
2\Gamma\hat{u} & & & & & & & & & & & & & \\
 & 2\gamma N\hat{u} & & & & & & & & & & & & -2\gamma\tilde{S}\hat{u} \\
 & & 2\gamma N\hat{u} & & & & & & & & & & & \\
 & & & \gamma(N-S_3)\hat{u} & & & & & & & & & & \\
 & & & & \gamma(N+S_3)\hat{u} & & & & & & & & & \\
 & & & & & 2\gamma\tilde{S}\hat{u} & & & & & & & & \\
 & & & & & & \gamma(N-S_3)\hat{u} & & & & & & & \\
 & -2\gamma\tilde{S}\hat{u} & & & & & & & & & & & & \gamma(N+S_3)\hat{u}
\end{bmatrix} , \tag{B3}$$

with all blank entries being zeros, and $\hat{u}$ is a 2×2 matrix:

$$\hat{u}=\begin{bmatrix}
\frac{1}{4} & \frac{i}{4} \\
-\frac{i}{4} & \frac{1}{4}
\end{bmatrix} , \tag{B4}$$

and $\tilde{S}=(S+S^*)/2$. In the matrix (B3), all rapidly oscillating correlations have been neglected; that is, we make the rotating-wave approximation with respect to the dissipative part of the evolution in the same sense as in Ref. [1]. Also, the same terms drop out from (B3) as a result of averaging over individual atomic phases φ_μ.

[1] J. Zakrzewski, M. Lewenstein, and T. M. Mossberg, first paper of this series, preceding paper, Phys. Rev. **44**, 7717 (1991).

[2] The experiment with an atomic beam is described in A. Lezama, Y. Zhu, M. Kanskar, and T. W. Mossberg, Phys. Rev. A **41**, 1576 (1990); experiment with a cell is described in G. Khitrova, J. F. Valley, and H. M. Gibbs, Phys. Rev. Lett. **60**, 1126 (1988).

[3] See also M. Lewenstein, Y. Zhu, and T. W. Mossberg, Phys. Rev. Lett. **64**, 3131 (1990).

[4] F. Bloch and A. J. F. Siegert, Phys. Rev. **57**, 522 (1940).

[5] H. Haken, *Laser Light Dynamics,* Vol. 2 of *Light* (North-Holland, Amsterdam, 1981); H. Haken, in *Encyclopedia of Physics,* 2nd corrected ed., edited by R. G. Lerner and G. L. Trigg (Springer, New York, 1984), Vol. XXV/2c.

[6] R. J. Glauber, in *Quantum Optics and Electronics,* edited by C. D. A. Blandin and C. Cohen-Tannoudji (Gordon and Breach, New York, 1965); Phys. Rev. Lett. **10**, 84 (1963); Phys. Rev. **130**, 2529 (1963); **131**, 2766 (1963); E. C. G. Sudarshan, Phys. Rev. Lett. **10**, 227 (1963).

[7] C. W. Gardiner, *Stochastic Methods for Physics, Chemistry, and the Natural Sciences* (Springer, Berlin, 1983).

[8] W. Weidlich and F. Haake, Z. Phys. **185**, 30 (1965); **186**, 203 (1965); H. Haken, F. Risken, and W. Weidlich, Z. Phys. **206**, 355 (1967); see also an alternative approach of M. O. Scully and W. E. Lamb, Jr., Phys. Rev. Lett. **16**, 853 (1966); Phys. Rev. A **166**, 246 (1968).

[9] L. A. Lugiato, F. Casagrande, and L. Pizzuto, Phys. Rev. A **26**, 3438 (1982); F. Casagrande, E. Eschenazi, and L. A. Lugiato, *ibid.* **29**, 239 (1984); F. Haake and M. Lewenstein, Z. Phys. B **48**, 37 (1982); Phys. Rev. A **27**, 1013 (1983).

[10] D. Stoler, Phys. Rev. D **1**, 3217 (1970); **4**, 1925 (1971).

[11] Special issue on squeezed states of the electromagnetic field, edited by H. J. Kimble and D. Walls, J. Opt. Soc. Am. B **4**, (1987); special issue on squeezed states, edited by

R. Loudon and P. L. Knight, J. Mod. Opt. **34** (1987).
[12] M. O. Scully, K. Wódkiewicz, M. S. Zubairy, J. Bergou, N. Lu, and J. Meyer ter Vehn, Phys. Rev. Lett. **60**, 1832 (1988).
[13] B. Yurke, Phys. Rev. A **29**, 408 (1984); M. Collet and C. W. Gardiner, *ibid.* **30**, 1386 (1984).
[14] For a review of recent results, see D. F. Walls, P. D. Drummond, A. S. Lane, M. A. Marte, M. D. Reid, and H. Ritsch, in *Squeezed and Nonclassical Light,* Proceedings of a NATO Advanced Research Workshop, edited by P. Tombesi and E. R. Pike (Plenum, New York, 1989), p. 1; L. A. Lugiato, M. Vadacchino, and F. Castelli, in *ibid.*, p. 161.
[15] J. Gea-Banacloche, N. Lu, L. M. Pedrotti, S. Prasad, M. O. Scully, and K. Wódkiewicz, Phys. Rev. A **41**, 369 (1990).
[16] M. Lax, Phys. Rev. **145**, 110 (1966); in *Physics of Quantum Electronics,* edited by P. L. Kelley *et al.* (McGraw-Hill, New York, 1966); see also Ref. [5].
[17] J. Zakrzewski, M. Lewenstein, and T. W. Mossberg, third paper of this series, following paper, Phys. Rev. A **44**, 7746 (1991).
[18] L. Mandel, Phys. Rev. Lett. **49**, 136 (1982); see also Refs. [11], [13], and [14].
[19] G. S. Agarwal, Phys. Rev. A **41**, 2886 (1990).
[20] G. S. Agarwal, Phys. Rev. A **42**, 686 (1990).